



Statistical analysis of nonlinear coupling in a WDM system over a two mode fiber

ABDERRAHMEN TRICHILI,^{1,2} MOURAD ZGHAL,^{1,3} LUCA PALMIERI,²
ANDREA GALTAROSSA,² AND MARCO SANTAGIUSTINA^{2,*}

¹University of Carthage, Engineering School of Communication of Tunis (SupCom), GreSCom Laboratory, Ghazala Technopark, 2083, Ariana, Tunisia

²Department of Information Engineering, University of Padova, Via Gradenigo 6/B, 35131 Padova, Italy

³Institut Mines-Télécom/Télécom SudParis, 9 rue Charles Fourier, 91011 EVRY, France

*marco.santagiustina@unipd.it

Abstract: We study the effect of nonlinear coupling in a WDM configuration over a two-mode fiber. A statistical analysis is presented that takes into account the effect of the random phase-sensitive amplification or depletion. Our results show high nonlinear coupling between the modes. We have quantified the channel power fluctuations, due to the wave phase random variations, at the output of the fiber. We also investigate the effect of random linear mode coupling on the nonlinear mode coupling.

© 2018 Optical Society of America under the terms of the [OSA Open Access Publishing Agreement](#)

OCIS codes: (060.4370) Nonlinear optics, fibers; (190.4380) Nonlinear optics, four-wave mixing; (060.0060) Fiber optics and optical communications.

References and links

1. D. J. Richardson, "Filling the light pipe," *Science* **30**, 327–328 (2010).
2. D. J. Richardson, J. M. Fini, and L. E. Nelson, "Space-division multiplexing in optical fibres," *Nat. Photonics* **7**, 354–362 (2013).
3. C. Koebele, M. Salsi, G. Charlet, and S. Bigo, "Nonlinear effects in mode division multiplexed transmission over few-mode optical fiber," *IEEE Photon. Technol. Lett.* **23**, 1316–1318 (2011).
4. A. Mecozzi, C. Antonelli, and M. Shtaif, "Nonlinear propagation in multi-mode fibers in the strong coupling regime," *Opt. Express* **20**, 11673–11678 (2012).
5. A. Mecozzi, C. Antonelli, and M. Shtaif, "Coupled Manakov equations in multimode fibers with strongly coupled groups of modes," *Opt. Express* **20**, 23436–23441 (2012).
6. S. Mumtaz, R.-J. Essiambre, and G. P. Agrawal, "Nonlinear propagation in multimode and multicore fibers: generalization of the Manakov equations," *J. Lightwave Technol.* **31**, 398–406 (2013).
7. C. Antonelli, M. Shtaif, and A. Mecozzi, "Modeling of nonlinear propagation in space-division multiplexed fiber-optic transmission," *J. Lightwave Technol.* **34**, 36–54 (2016).
8. R. H. Stolen, J. E. Bjorkholm, and A. Ashkin, "Phase-matched three wave mixing in silica fiber optical waveguides," *App. Phys. Lett.* **24**, 308–310 (1974).
9. F. Poletti and P. Horak, "Description of ultrashort pulse propagation in multimode optical fibers," *J. Opt. Soc. Am. B* **25**, 1645–1654 (2008).
10. F. Poletti and P. Horak, "Dynamics of femtosecond supercontinuum generation in multimode fibers," *Opt. Express* **17**, 6134–6147 (2009).
11. A. Ben Salem, A. Trichili, R. Cherif, and M. Zghal, "Rigorous study of supercontinuum generation in few mode fibers," *Appl. Opt.* **16**, 4317–4322 (2016).
12. R. J. Essiambre, R. Ryf, M. A. Mestre, A. H. Gnauck, R. W. Tkach, A. R. Chraplyvy, Y. Sun, X. Jiang, and R. Lingle Jr, "Experimental investigation of inter-modal four-wave mixing in few-mode fibers," *IEEE Photon. Technol. Lett.* **25**, 539–541 (2013).
13. Y. Xiao, R. J. Essiambre, M. Desgroesilliers, A. M. Tulino, R. Ryf, S. Mumtaz, and G. P. Agrawal, "Theory of intermodal four-wave mixing with random linear mode coupling in few-mode fibers," *Opt. Express* **22**, 32039–32059 (2014).
14. M. Esmaelpour, R. J. Essiambre, N. Fontaine, R. Ryf, J. Toulouse, Y. Sun, and R. Lingle, "Power fluctuations of inter-modal four-wave mixing in few-mode fibers," *J. Lightwave Technol.* **35**, 2429–2435 (2017).
15. M. Guasoni, F. Parmigiani, P. Horak, J. Fatome, and D. J. Richardson, "Intermodal four-wave mixing and parametric amplification in kilometer-long multimode fibers," *J. Lightwave Technol.* **35**, 5296–5305 (2017).
16. W. Pan, Q. Jin, X. Li, and S. Gao, "All-optical wavelength conversion for mode-division multiplexing signals using four-wave mixing in a dual-mode fiber," *J. Opt. Soc. Am. B* **32**, 2417–2424 (2015).

17. A. Trichili, M. Zghal, L. Palmieri, and M. Santagiustina, "Phase-sensitive mode conversion and equalization in a few mode fiber through parametric interactions," *IEEE Photon. J.* **9**, 1–10 (2017).
18. I. Neokosmidis, T. Kamalakis, A. Chipouras, and T. Spicopoulos, "New techniques for the suppression of the four-wave mixing-induced distortion in nonzero dispersion fiber WDM systems," *J. Lightwave Technol.* **23**, 1137–1144 (2005).
19. P. Poggiolini, "The GN model of non-linear propagation in uncompensated coherent optical systems," *J. Lightwave Technol.* **30**, 3857–3879 (2012).
20. V. Curri, A. Carena, P. Poggiolini, G. Bosco, and F. Forghieri, "Extension and validation of the GN model for non-linear interference to uncompensated links using Raman amplification," *Opt. Express* **21**, 3308–3317 (2013).
21. R. Dar, M. Feder, A. Mecozzi, and M. Shtaif, "Properties of nonlinear noise in long, dispersion-uncompensated fiber links," *Opt. Express* **21**, 25685–25699 (2013).
22. O. Golani, R. Dar, M. Feder, A. Mecozzi, and M. Shtaif, "Modeling the bit-error-rate performance of nonlinear fiber-optic systems," *J. Lightwave Technol.* **34**, 3482–3489 (2016).
23. C. Antonelli, O. Golani, M. Shtaif, and A. Mecozzi, "Nonlinear interference noise in space-division multiplexed transmission through optical fibers," *Opt. Express* **25**, 13055–13078 (2017).
24. M. Eiselt, "Limits on WDM systems due to four-wave mixing: a statistical approach," *J. Lightwave Technol.* **17**, 2261–2267 (1999).
25. S. Betti, M. Giaconi, and M. Nardini, "Effect of four-wave mixing on WDM optical systems: a statistical analysis," *IEEE Photon. Technol. Lett.* **15**, 1079–1081 (2003).
26. J. Hansryd, P. A. Andrekson, M. Westlund, J. Li, and P. O. Hedekvist, "Fiber-based optical parametric amplifiers and their applications," *IEEE J. Sel. Top. Quantum Electron.* **8**, 506–520 (2002).
27. Q. Lin and G. P. Agrawal, "Vector theory of four-wave mixing: polarization effects in fiber-optic parametric amplifiers," *J. Opt. Soc. Am. B* **21**, 1216–1224 (2004).
28. L. Gruner-Nielsen, Y. Sun, J. W. Nicholson, D. Jakobsen, K. G. Jespersen, R. Lingle, and B. Palsdottir, "Few mode transmission fiber with low DGD, low mode coupling, and low loss," *J. Lightwave Technol.* **30**, 3693–3698 (2012).
29. M. Zelen and N. C. Severo, "Probability function," in *Handbook of Mathematical Functions*, M. Abramowitz and I. Stegun, eds., Vol. 55 of Applied Mathematics Series (National Bureau of Standards, 1964), ch. 26, pp. 926–976.
30. L. Palmieri, "Coupling mechanism in multimode fibers," *Proc. SPIE* **9009**, 90090G (2013).
31. L. Palmieri and A. Galtarossa, "Coupling effects among degenerate modes in multimode optical fibers," *IEEE Photon. J.* **6**, 1–8 (2014).
32. P. K. A. Wai and C. R. Menyuk, "Polarization mode dispersion, decorrelation, and diffusion in optical fibers with randomly varying birefringence," *J. Lightwave Technol.* **14**, 148–157 (1996).

1. Introduction

The continuous growth of capacity demand might push the actual communication systems into a bandwidth bottleneck. Space is an additional degree of freedom in optical fiber communications that can be exploited as a solution to cope with the foreseen capacity crunch [1, 2]. This has focused a considerable interest towards a new research area known as space division multiplexing (SDM). With the emergence of SDM, nonlinearity of different kinds have been studied in few mode fibers (FMFs) [3–7]. A particular nonlinear effect is four wave mixing (FWM), which has been demonstrated during the 70ies in multimode fibers [8]. So far, FWM has been reported over short photonic crystal fibers and found to be responsible for energy transfer between degenerate modes [9–11]. In step and graded index FMFs, FWM has been theoretically and experimentally investigated [12–15], and the potential of FWM for wavelength conversion has been highlighted [16]. In particular, in [14] large power fluctuations have been highlighted in the case of wavelength conversion. Phase insensitive and phase sensitive amplification (PIA, PSA) have been recently studied and analytical formulas under the undepleted pump approximation were found [17].

In wavelength division multiplexing (WDM) over single mode fibers, FWM is known to be deleterious because 50 GHz spaced channels can be phase matched in nonzero dispersion fibers and FWM has detrimental effects by causing interchannel-crosstalk and channel power imbalance [18]. In long-haul WDM systems the effects of nonlinearity have been often considered in terms of a nonlinear interference noise with different models [19–22]. In the context of FMFs, the effects of the nonlinearity have been considered in the frame of the Manakov equations valid for strong mode coupling [4, 5, 7] which, in a WDM scenario, also lead to the definition of a nonlinear interference noise [23]. Noticeably, phase matching conditions between waves on the

same mode are mostly avoided in FMFs because the dispersion coefficient is of the same order of that of single-mode fibers ($\approx 20 \text{ ps}^2/\text{km}$); however, it can be fulfilled between a set of waves on different modes.

In this work, we are interested in the effect of FWM in a WDM configuration over a fiber propagating two families of modes: LP_{01} (two degenerate modes, respectively, polarized along x and y axes) and LP_{11} (four degenerate modes, defined by two orthogonal azimuthal eigenfunctions which identify the sub-families LP_{11a} and LP_{11b} and two polarizations for each sub-family). We focus the attention on the impact of FWM between channels and in particular, we present the effect due to the channel phases which must be considered as random variables. This effect has been pointed out and studied in single mode fibers [24, 25] but, to the best of our knowledge, has not yet received attention in SDM. A statistical approach shows that input phase fluctuations are transformed into output power fluctuations bounded between predictable maximum and minimum values, with a high dynamic range, in particular for low power channels. Our analysis includes also the effect of random linear mode coupling due to the residual birefringence and the core ellipticity. When linear mode coupling is included, we observe a reduction of the efficiency of the nonlinear effects, consistently with what found by Antonelli *et al.* in [23].

However, in this work, differently from [23], we will not consider the nonlinear noise (due to self-phase, cross-phase modulation and FWM) over a WDM system for long propagation distances in the strong coupling regime, but rather we will point out and quantify the specific cross-talk that occurs at the beginning of the propagation when the channel powers are large and FWM comparably efficient to weak linear coupling. When the channel power becomes too low this cross-talk vanishes but the power fluctuations accumulated up to that point remain. Moreover, the statistical analysis considering the linear coupling contribution reveals that modes generated by mode coupling have remarkably different output powers.

2. Theoretical model

The WDM system is composed by 50 GHz-spaced channels as illustrated by Fig. 1. At each frequency it is possible to have two channels by launching both LP_{01} and LP_{11} modes. There are three conservation conditions to be met for FWM interaction to occur: the conservation of the photon number, the photon momentum and the photon angular-momentum [26, 27]. In the WDM scenario of Fig. 1, because of the constant frequency detuning between channels, the first condition is met by several groups of four waves, similarly to SMFs [24]. The conservation of photon momentum entails the minimization of the linear phase mismatch [26] defined by

$$\Delta\beta^{(mnop)} = \beta^{(m)}(\omega_i) + \beta^{(n)}(\omega_j) - \beta^{(o)}(\omega_k) - \beta^{(p)}(\omega_l) \quad (1)$$

where $\beta^{(p)}(\omega_l)$ is the propagation constant of mode p ($p = 01$ or $p = 11$) at frequency ω_l , which can be approximated by a Taylor expansion around an arbitrary frequency ω_0 :

$$\beta^{(p)}(\omega_l) \approx \beta_0^{(p)} + \beta_1^{(p)} \Delta\omega_l + \frac{1}{2} \beta_2^{(p)} \Delta\omega_l^2 + \dots \quad (2)$$

The dispersion coefficients $\beta_i^{(p)} = \partial^i \beta^{(p)} / \partial \omega^i$ ($i = 0, 1, 2, \dots$) are calculated at ω_0 and $\Delta\omega_l = \omega_l - \omega_0$. The expansion in eq. 2 can be truncated at the second order as shown in [12], because high order dispersion terms are negligible in comparison to the first two. The value of $\Delta\beta^{(mnop)}$ depends on the fiber design, therefore, in order to quantify the actual efficiency of each FWM interaction we need to define the specific fiber.

We considered the graded index fiber defined in [28]; linear coupling smaller than -25 dB for a 30 km length is reported for this fiber. The parameters of the fiber, at $\lambda_0 = 1550 \text{ nm}$ are: differential group delay (DGD) $\beta_1^{\text{LP}11} - \beta_1^{\text{LP}01} = -81 \text{ ps/km}$, group velocity dispersion (GVD) coefficients $\beta_2^{\text{LP}11} = -25.509 \text{ ps}^2/\text{km}$ and $\beta_2^{\text{LP}01} = -25.254 \text{ ps}^2/\text{km}$. Loss coefficients are

slightly mode dependent $\alpha_{LP_{01}} = 0.198$ dB/km and $\alpha_{LP_{11}} = 0.191$ dB/km. The knowledge of the dispersion coefficients enables the determination of the phase mismatch [Eq. (1)], for all the possible combinations of four waves on the WDM grid. It is found that there exists only one combination that gives $\Delta\beta^{(mnop)} \simeq 0$, which entails the interaction of a wave at frequency $\omega_1/(2\pi) = 192.1$ THz propagating on a LP_{11} family mode (hereinafter defined as channel 1), a wave at $\omega_4/(2\pi) = 193.1$ THz on a LP_{01} family mode (channel 4) and two waves at the intermediate frequency $(\omega_1 + \omega_4)/(4\pi) = 192.6$ THz, one propagating on a LP_{01} mode (channel 2) and one on a LP_{11} mode (channel 3). Note that a similar configuration could be found also for the fiber defined in [12] and this seems to indicate that this can be a property of several FMFs.

The last condition to be satisfied (angular momentum conservation) corresponds to a polarization selection rule among waves, i.e. the waves interact if they have the same polarization either in two groups of two waves or in one group of four waves [27]. Here, we assume to launch linearly polarized waves and the selection rule (see [27] for details) imposes all four waves to have the same polarization (say x). Under the assumption of negligible linear mode coupling and

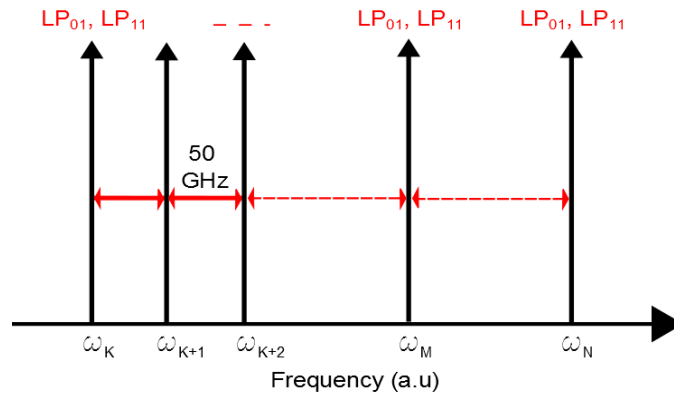


Fig. 1. System configuration: the WDM channels are spaced by 50 GHz in the C band on both LP_{01} and LP_{11} modes.

in the continuous wave approximation (CW), the equations describing the propagation of the four channels are those given by Stolen *et al.* [8]:

$$\begin{aligned}
 -i \frac{dA_1}{dz} &= i \frac{\alpha_1}{2} A_1 + \gamma (f_{1111} |A_1|^2 A_1 + 2 \sum_{n,n \neq 1} f_{11nn} |A_n|^2 A_1 + 2 f_{1234} A_2 A_3 A_4^* \exp(i\Delta\beta z)) \\
 -i \frac{dA_2}{dz} &= i \frac{\alpha_2}{2} A_2 + \gamma (f_{2222} |A_2|^2 A_2 + 2 \sum_{n,n \neq 2} f_{22nn} |A_n|^2 A_2 + 2 f_{2143} A_1 A_4 A_3^* \exp(-i\Delta\beta z)) \\
 -i \frac{dA_3}{dz} &= i \frac{\alpha_3}{2} A_3 + \gamma (f_{3333} |A_3|^2 A_3 + 2 \sum_{n,n \neq 3} f_{33nn} |A_n|^2 A_3 + 2 f_{3142} A_1 A_4 A_2^* \exp(-i\Delta\beta z)) \\
 -i \frac{dA_4}{dz} &= i \frac{\alpha_4}{2} A_4 + \gamma (f_{4444} |A_4|^2 A_4 + 2 \sum_{n,n \neq 4} f_{44nn} |A_n|^2 A_4 + 2 f_{4231} A_2 A_3 A_1^* \exp(i\Delta\beta z)) \quad (3)
 \end{aligned}$$

where $A_n(z)$ are the complex envelopes of the interacting channels ($n = 1, 2, 3, 4$), α_k is the linear loss coefficient of channel k and $\gamma = 1.128 \text{ W}^{-1} \text{ km}^{-1}$ is the nonlinear coefficient. The coefficients f_{ijkl} denote the normalized mode overlap integrals [8, 13]: f_{iiii} apply to the self-phase modulation (SPM), f_{iinn} to the cross-phase modulation (XPM) while f_{ijkl} to the FWM. The corresponding values calculated for the studied fiber are:

$$f_{ijkl} = \begin{cases} 1 & \text{for 4 waves in LP}_{01} \text{ or LP}_{11a} \text{ or LP}_{11b} \\ 0.702 & \text{for 2 waves in LP}_{01} \text{ and 2 waves in LP}_{11a} \text{ or LP}_{11b} \\ 0.493 & \text{for 2 waves in LP}_{11a} \text{ and 2 waves in LP}_{11b} \\ 0 & \text{for all other cases} \end{cases} \quad (4)$$

Finally, $\Delta\beta = \beta^{11}(\omega_1) + \beta^{01}(\omega_4) - \beta^{11}(\omega_2) - \beta^{01}(\omega_2) (\approx 0)$ is the linear phase mismatch; it appears in the argument of the last exponentials because each wave phase was referenced to the respective mode phase delay $\beta^{(p)}z$ [8].

3. Nonlinear model implementation

3.1. Analysis

We start by investigating the effect of nonlinear coupling on the propagating waves, i.e. neglecting linear coupling; in this way we can evaluate the strength of the nonlinear coupling alone. The resolution of the coupled equations [Eq. (3)] is performed using a Runge-Kutta algorithm. Let us consider to launch the waves in channels 1, 2 and 4, all with the same input power of +10 dBm. The aim of this calculation is to determine the strength of the nonlinear coupling to channel 3, i.e. the ratio $|A_3(z)|^2/|A_2(z=0)|^2 = P_3(z)/P_2(z=0)$ which in FWM terminology, is defined as the signal-to-idler conversion efficiency.

The results of the integration are shown in Fig. 2. We observe that the conversion efficiency

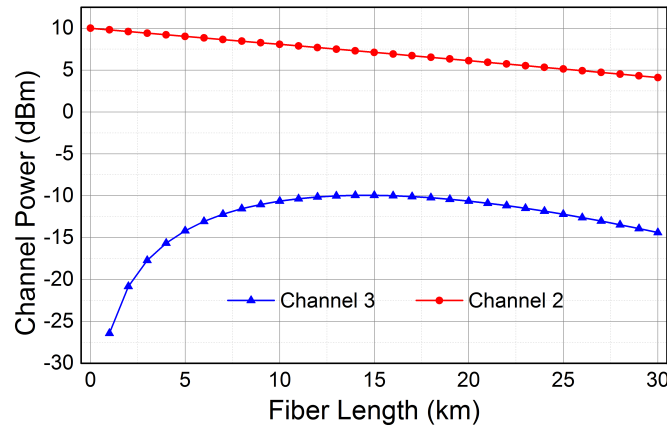


Fig. 2. Channel power evolution when mode LP₁₁ at frequency ω_2 (channel 3) is not launched.

increases with the propagation distance up to about 15 km where it reaches -20 dB. At 30 km, the coupling (≈ -24 dB) is comparable to the linear coupling reported by L. Gruner-Nielsen *et al.* in [28].

Note that these results were obtained by taking into account only 4 waves on 3 wavelengths. However, we checked that the differences with respect to the case when all 21 channels are considered (which entailed the resolution of 42 nonlinearly coupled equations with 2 modes per frequency) are negligible, since all other interactions are essentially mismatched. Figures 2 and 3 clarify also that the FWM nonlinear interaction takes place in the initial stage of propagation, when the channels are still enough powerful, and then it becomes negligible. Therefore, the effect of power exchange/conversion has affected permanently the various channels. By launching all four waves, with the same input power, the results of Fig. 3 are obtained, where we observe that channel 2 and channel 3 are amplified while the other two (channel 1 and channel 4) are depleted with respect to the case when no FWM occurs between the waves (dashed lines in Fig. 3).

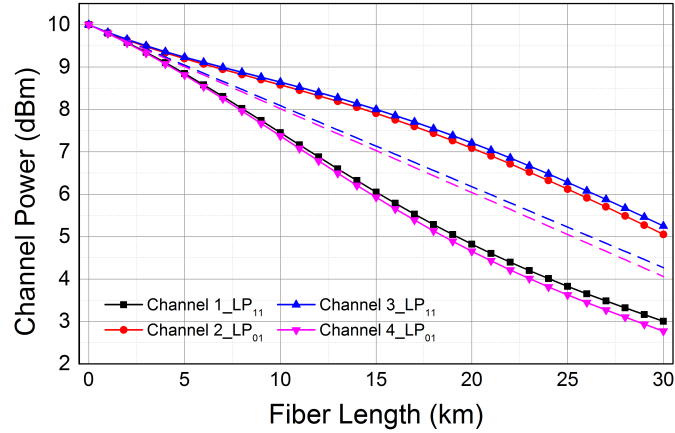


Fig. 3. Channel power evolution for equal channel input powers of 10 dBm. Solid lines with marker correspond to the case in which FWM is considered, while dashed lines are obtained without FWM (losses only).

The occurrence of amplification or depletion is dictated by the phase mismatch term $\Delta\beta$ and by the relative phase among the waves, that is fixed at the input for the results of Fig. 3 [17]. This dependence can be derived from the power evolution equations as a function of the longitudinal coordinate z which can be expressed as follows (see also [26]):

$$\begin{aligned}\frac{dP_{1,4}}{dz} &= \frac{dA_{1,4}}{dz} A_{1,4}^* + \frac{dA_{1,4}^*}{dz} A_{1,4} \\ &= -\alpha P_{1,4} - 4\sqrt{P_1 P_2 P_3 P_4} \sin(\Phi) \\ \frac{dP_{2,3}}{dz} &= \frac{dA_{2,3}}{dz} A_{2,3}^* + \frac{dA_{2,3}^*}{dz} A_{2,3} \\ &= -\alpha P_{2,3} + 4\sqrt{P_1 P_2 P_3 P_4} \sin(\Phi)\end{aligned}\quad (5)$$

where $\Phi = \Delta\beta z + \phi_2 + \phi_3 - \phi_1 - \phi_4$, $P_k = |A_k|^2$ is the power of channel k while ϕ_k is its phase. The depletion or amplification behaviour depends on the sign of $\sin(\Phi)$, which is essentially determined by the initial condition on the channel phases. In fact the evolution of Φ is well approximated by [26]:

$$\frac{d\Phi}{dz} \simeq \Delta\beta + \gamma(P_1 + P_4 - P_2 - P_3) \simeq 0 \quad (6)$$

because $\Delta\beta \simeq 0$ and the second term is also very small (of the order of 10^{-3} km^{-1}) and of opposite sign with respect to the first. The effect of the input phases of the channels on the output power can be observed in Fig. 4, where we fixed the phases of two channels ($\phi_1 + \phi_4 = \pi/2$) and we varied $\phi_2 + \phi_3$.

From Fig. 4, we observe that the power of each channel can actually fluctuate by more than 2 dB simply because of a different relative phase relation among the channels at input. The input phases of WDM channels are random variables under the hypothesis that each wavelength uses a different laser source. Thus, the next step will be to perform a statistical analysis of channel fluctuations considered as random variables.

3.2. Statistical analysis: effect of the channel phases

We quantify the statistics of the channel power fluctuations by supposing that the phases of channel 1 and channel 4 are independent and identically distributed random variables following a

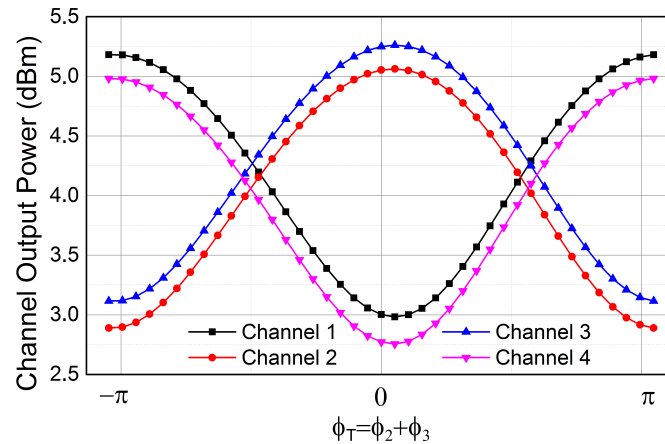


Fig. 4. Channel output power as a function of input phases for equal channel input powers of 10 dBm.

uniform distribution over the range $[0, 2\pi]$. Since a single laser can be used to launch channel 2 and channel 3 on the same frequency and two distinct modes, we assume that both channels have the same phase, that is fixed as a reference. We can also assume that the input phase relation is maintained during the coherence time of the lasers which can be estimated to be about $2 \mu\text{s}$ for a laser linewidth of about 500 kHz. For a 10 Gb/s channel this means that the phase coherence is maintained over about 20 thousands bit time slots. In FMFs the walk-off effect must be also taken into consideration and the bit sequences will walk-off completely at a distance of $2\mu\text{s}/81\text{ps/km} \approx 25 \cdot 10^3 \text{ km}$, well beyond the range over which FWM is effective. Therefore, the CW approach we used is expected to yield the average interaction at least for on-off keying (OOK) systems. In coherent systems the effects will be more complicated as the phase is also modulated at input.

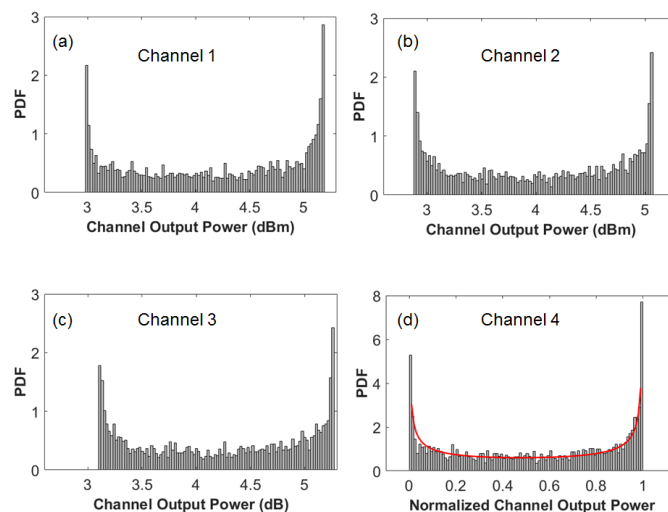


Fig. 5. PDF (over 3000 independent realizations) of the four channels for equal input channel powers.

The probability density functions (PDFs) of channel powers are limited between the maximum and minimum values obtained in Fig. 4 and are presented in Fig. 5 for each channel involved in the FWM. In Figs. 5(a-c) we present the PDFs as functions of the output power, while in Fig. 5(d), in order to fit the results with a known PDF, we normalized the output channel power between 0 and 1 (to show its range of variation). The calculated PDF is well fitted by a beta distribution with $a = 0.49$, $b = 0.44$ as shown in Fig. 5(d). We recall that the PDF of a beta distribution with parameters $a, b > 0$ is ($0 \leq x \leq 1$) [29]

$$f(x; a, b) = \frac{1}{B(a, b)} x^{a-1} (1-x)^{b-1}, \quad (7)$$

where B is the Beta function. The beta distribution (which includes the uniform distribution as a special case when $a = b = 1$), characterizes random variables defined, like in this case, within a bounded interval. The results of Fig. 5 can be therefore explained by observing that the uniform distribution of Φ is altered by the sine function in Eqs. 5 and that values $\Phi \approx 0$ implies $\sin(\Phi) \approx 0$ so that no power transfer occurs. The parameters of the fitting function were calculated and were slightly different from one channel to the other due to the difference between linear mode losses. The fluctuations of the output channel power are bounded by the phase-sensitive extinction ratio (PER) which quantifies the dynamic range of the phase sensitive amplification/depletion. Exact formulas for the PER were determined under the undepleted pump approximation in [17] and one of the main result found in that work is the dependence of the PER on the input power unbalance between the waves. Therefore, we also studied the case when channel 3 presents an input power of -10 dBm.

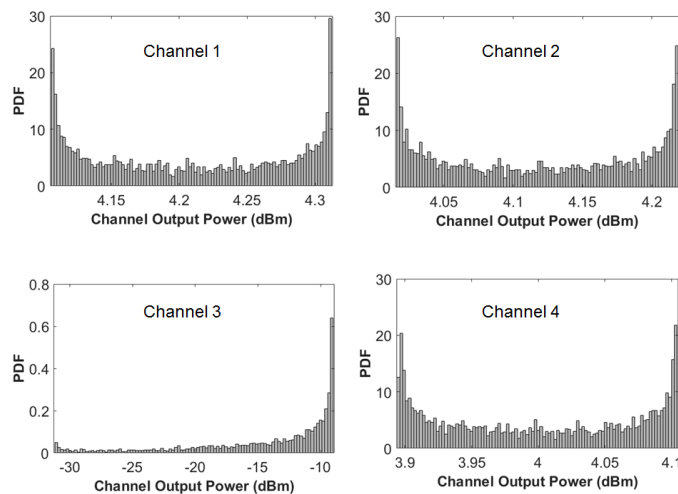


Fig. 6. PDF (over 3000 independent realizations) of the four channels with -10 dBm for channel 3 as input power while the input power is +10 dBm for the other channels.

From the histograms depicted in Fig. 6, we can clearly observe that high-power channels are weakly affected. However, in the weak power channel, the fluctuations exceed 20 dB with a maximum probability around higher output powers. This is an effect of the conservation of the photon number which entails a large depletion of low power waves because of the interaction with high power ones [17]. From this analysis one should conclude that interactions of bits of an OOK system with a high level in all four channels are efficient and lead to significant random power fluctuations; nevertheless, if at least one bit is at the low level the interaction leads to negligible (or even positive, because the power of the low level is depleted) effects.

The next step of the analysis is to include random linear mode coupling to the modeling and determine its effect on the channel power evolution and on the power PDFs.

4. Linear coupling effects

In FMFs, random linear mode coupling can be induced by different physical effects such as bending, stress, twisting, rotation, pressures and fiber core shape or refractive index imperfections. We adopt

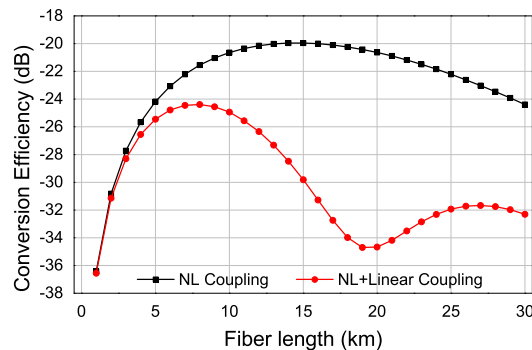


Fig. 7. Conversion efficiency for channel 3 in the case of nonlinear coupling only (black squares) and linear and nonlinear coupling (red dots).

a model which takes into account core ellipticity and random birefringence following [30, 31], as these are the two sources of coupling that are intrinsic to the fiber (i.e. not necessarily induced by the external environment). The model accounts for coupling through a coupling matrix K that, at each frequency, couples six mode envelopes $\vec{A} = [A_{01x}, \dots, A_{11by}]$ within the same mode family according to the equation $d\vec{A}/dz = -iK\vec{A}$. The key element of the model is the angle θ describing the orientation of the perturbation. Though all details of the model can be found in [31], here we just recall that birefringence and core ellipticity (i.e. the perturbation strength) are assumed to be constant along the fiber. Differently, the local axes of birefringence and of core ellipse (i.e. the perturbation orientation) are assumed to be parallel and to vary at random with the propagation direction z , according to a Wiener process: $d\theta/dz = -\eta(z)/L_F$, where $\eta(z)$ is a zero mean Gaussian white noise with autocorrelation $r_\eta = \delta(z)$ and L_F is the correlation length [32]. For the simulations, we fixed $L_F = 30$ m, the birefringence $\Delta_n = 10^{-6}$ and the maximum ratio between maximum core radius variation and the core radius, $r_e = 10^{-3}$.

We first compare the conversion efficiency of the same realization of Fig. 2 with and without random linear mode coupling. Results, depicted in Fig. 7, show that the effect of linear coupling is to reduce the effectiveness of the FWM and to introduce additional power fluctuations. This is consistent with what found by Antonelli et al. in [23] and an additional efficiency decrease might be expected when applying perturbations that also introduce coupling among different mode families. We can clearly see from Fig. 8 that when linear mode coupling is included in the modeling, channel powers are reduced comparing to the case when only nonlinear effects are considered. Missing power is transferred to the other modes and so FWM efficiency decreases. We should point out that no power is transferred to channel 3 when we only take into consideration random linear mode coupling without any nonlinear term. We additionally perform the statistical analysis of the phase dependence in presence of the linear coupling. The PDFs of the output power are shown in Fig. 9. We can see that the dynamic range of the channel output power has been reduced to about 1.1 dB for the case in which equal power is launched in all channels. This confirms the general trend of linear coupling to decrease nonlinear effects though not completely

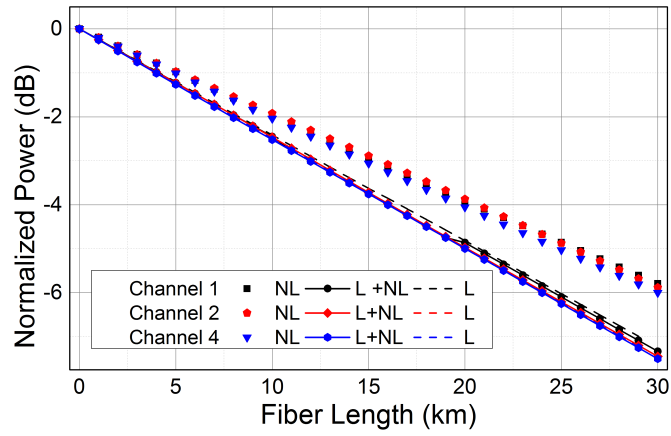


Fig. 8. Comparison between three cases of channel power evolution. Markers represent the channel powers with nonlinear coupling only, solid lines with marker, correspond to channel powers with linear and nonlinear effects and finally dashed lines are the powers when only linear coupling is included in the modeling.

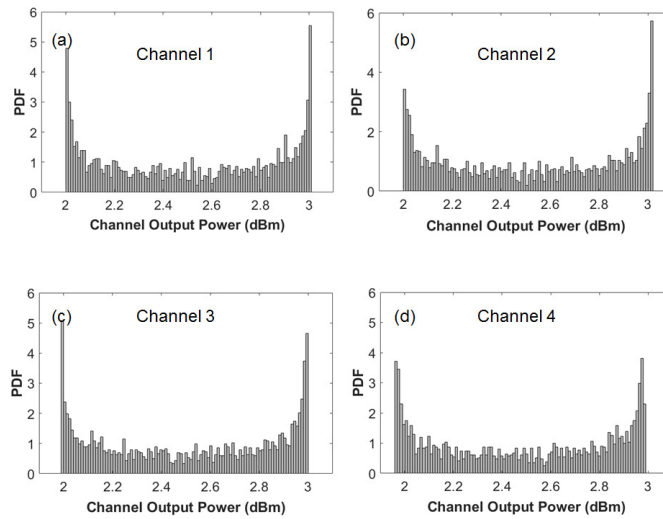


Fig. 9. PDF (over 3000 independent realizations) of the four channels for equal input channel powers.

deleting the results of an efficiently phase-matched FWM. The PDF for channel 2 and channel 4, launched over LP_{01} mode on polarization x, follows again a beta distribution function but with different parameters with respect to the case without linear coupling ($a = 0.28$ and $b = 0.34$ for the case of channel 2). For channel 1 and channel 3, launched over LP_{11a} mode on polarization x, the PDF tends to follow a beta distribution function as well (with $a = 0.248$ and $b = 0.321$ calculated for channel 3).

We finally present in Fig. 10 the PDF of the modes that have been generated by the linear coupling. Power from the initially launched modes have been only transferred to 8 among the 14 possible modes. This is due to the fact that coupling due to birefringence and core ellipticity could only occur between modes within the same mode family over the same frequency [31]. We observe that the output power levels are widely different between modes (around -68 dBm for mode LP_{01y} at ω_2 and around -10 dBm for mode LP_{11bx} at frequencies ω_1 and ω_2). The difference is explained by the fact that waves launched on LP_{01x} at ω_2 , LP_{01x} at ω_3 , LP_{11bx} at ω_1 and LP_{11bx} at ω_2 are phase matched. Therefore the nonlinear interaction between the waves leads to a reinforcement of that particular mode set. Fluctuations are again in the order of 1 dB for the most intense modes and the statistical distribution is fitted by a beta distribution function of parameters $a = 0.33$ and $b = 0.377$ (calculated for LP_{01y} at frequency ω_3).

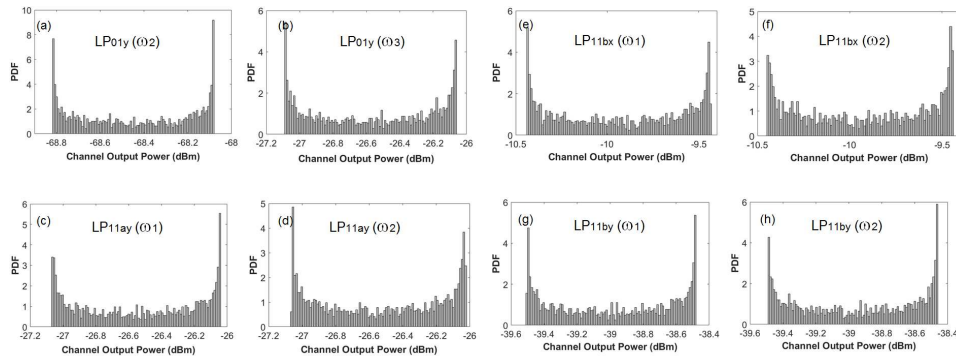


Fig. 10. PDF (over 3000 independent realizations) of the channels generated by random linear coupling.

5. Conclusion

In summary, we investigated the effects of linear and nonlinear coupling between signals launched on the LP_{01} and LP_{11} modes of a two mode fiber in a WDM scenario. After calculating the nonlinear coefficients of a few mode fiber, we verified that the strength of FWM is comparable with that of the linear coupling, in the initial stage of propagation. The combined effects of linear and nonlinear coupling can therefore lead to changes of the signal power that are significant for a WDM communication system. In particular, we considered the effect of the wave phases, which in FWM dictate whether amplification or depletion of the waves occur. Input phase fluctuations, which evolve over the coherent time of the different laser sources, are therefore transformed into amplitude fluctuations by the FWM. We have statistically studied the combined effects of linear and nonlinear coupling that are responsible for wave power unbalance and fluctuations. Linear coupling generally reduces fiber nonlinearity effects. The statistical analysis in the presence of linear mode coupling showed the reduction of the power fluctuations. Conversely, nonlinear mode coupling can reinforce power transfer and fluctuations in modes that are generated by linear coupling. This work underline that in a WDM systems in few mode fibers there might exist a few set of (phase matched) channels which are highly influenced in the initial stage of propagation by

the four wave mixing, and that linear coupling can smooth this interaction but not cancel it. As well, linear coupling can be reinforced by nonlinear mixing giving rise to power fluctuations in linearly coupled modes.

Funding

Department of Information Engineering, University of Padova; Engineering School of Communication of Tunis (SupCom); Department of Information Engineering, University of Padova (Project Photon1).

Acknowledgments

We thank OFS for providing the FMF data. This research was carried out under the agreement between the Department of Information Engineering, University of Padova and the Engineering School of Communication of Tunis (SupCom). A. Trichili was funded by the Department of Information Engineering, University of Padova, Project Photon1.